Review Article

3D printed anatomical (bio)models in spine surgery: clinical benefits and value to health care providers

William C. H. Parr[1,2,3], Joshua L. Burnard[1,3], Peter John Wilson[4], Ralph J. Mobbs[1,3,4]

[1]Surgical and Orthopaedic Research Laboratories (SORL), Prince of Wales Clinical School, Faculty of Medicine, University of New South Wales (UNSW), Sydney, Australia; [2]3DMorphic Pty Ltd, Sydney, Australia; [3]NeuroSpine Surgery Research Group (NSURG), Sydney, Australia; [4]Department of Neurosurgery, Prince of Wales Private, Sydney, Australia

Contributions: (I) Conception and design: WCH Parr, RJ Mobbs; (II) Administrative support: RJ Mobbs; (III) Provision of study materials or patients: WCH Parr, PJ Wilson, RJ Mobbs; (IV) Collection and assembly of data: WCH Parr, JL Burnard, RJ Mobbs; (V) Data analysis and interpretation: WCH Parr, RJ Mobbs; (VI) Manuscript writing: All authors; (VII) Final approval of manuscript: All authors.

Correspondence to: Dr. William C. H. Parr, PhD. Surgical and Orthopaedic Research Laboratories (SORL), Level 1 Clinical Sciences Bld, Gate 6 Prince of Wales Hospital, UNSW, Avoca St, Randwick, Sydney, NSW 2031, Australia. Email: w.parr@unsw.edu.au.

Abstract: The applications of three-dimensional printing (3DP) for clinical purposes have grown rapidly over the past decade. Recent advances include the fabrication of patient specific instrumentation, such as drill and cutting guides, patient specific/custom long term implants and 3DP of cellular scaffolds. Spine surgery in particular has seen enthusiastic early adoption of these applications. 3DP as a manufacturing method can be used to mass produce objects of the same design, but can also be used as a cost-effective method for manufacturing unique one-off objects, such as patient specific models and devices. Perhaps the first, and currently most widespread, application of 3DP for producing patient specific devices is the production of patient specific anatomical models, often termed biomodels. The present manuscript focuses on the current state of the art in anatomical (bio)models as used in spinal clinical practice. The biomodels shown and discussed include: translucent and coloured models to aid in identification of extent and margins of pathologies such as bone tumours; dynamic models for implant trial implantation and pre-operative sizing; models that can be disassembled to simulate surgical resection of diseased tissue and subsequent reconstruction. Biomodels can reduce risk to the patient by decreasing surgery time, reducing the probability of the surgical team encountering unexpected anatomy or relative positioning of structures and/or devices, and better pre-operative planning of the surgical workflow including ordered preparation of the necessary instrumentation for multi-step and revision procedures. Conversely, risks can be increased if biomodels are not accurate representations of the anatomy, which can occur if MRI/CT scan data is simply converted into 3DP format without interpretation of what the scan represents in terms of patient anatomy. A review and analysis of the cost-benefits of biomodels shows that biomodels can potentially reduce cost to health care providers if operating room time is reduced by 14 minutes or more.

Keywords: 3D printing (3DP); patient specific; custom; computational anatomy; biomodel

Submitted Dec 16, 2019. Accepted for publication Dec 18, 2019.
doi: 10.21037/jss.2019.12.07
View this article at: http://dx.doi.org/10.21037/jss.2019.12.07

Introduction

Three-dimensional printing (3DP), also known as rapid prototyping, enables the physical realisation of virtual 3D Computer Aided Design (CAD) models. 3DP is an additive manufacturing process that builds a 3D object layer by layer, enabling the production of complex geometrical structures that would not be manufacturable using other

methods. Technological advancements in 3DP to medical-grade standards (such as printable biocompatible materials and printed part precision) in conjunction with improved resolution of patient imaging modalities, have recently catalysed a rapid expansion of biomedical 3DP applications in clinical, and particularly surgical, practice (1,2).

3DP is now commonly used to produce patient specific drill guides (3-6) and devices, which have been the focus of a number of recent case studies, case series and reviews (7-9). For the current manuscript, we focus on the precursor to, and typically workflow foundation of, these recent developments: virtual and haptic patient specific anatomical models, often termed biomodels (10).

Historically surgeons have predominantly relied on two-dimensional (2D) analyses of planar X-ray, CT and/or MRI images. 3D spatial-appreciation and interpretation of complex patho-anatomies is inherently limited by such 2D representation. Anatomical biomodelling, including the creation of a haptic construct that replicate the geometrical form of a biological structure by 3DP, offers a means to overcome these limitations as surgeons can manipulate a replica of a patient's anatomy. Although sometimes technically feasible through conventional manufacturing methods (such as casting or subtractive manufacturing), 3DP is unmatched as a manufacturing method in terms of time and resource requirements necessary to create accurate and intricate patient-specific anatomical models (11).

Aims

The present manuscript aims to discuss, with examples of anatomical models used in recent clinical cases, the production, clinical benefits and value of anatomical (bio) models in spine surgery.

Anatomical (bio)model use in spine surgery; brief history

In preliminary applications of anatomical models for surgical spine management by D'Urso *et al.* in 1999 (10), patient-specific biomodels were utilised to provide visual and tactile appreciation bony anatomy as well as aid assessment and understanding of pathology. Since then, biomodels have had wider application in the preoperative workflow, allowing surgeons to acquaint themselves with the unique anatomical complexities of the presenting case by visualisation and tactile manipulation of an anatomical replicate (12). This process has been demonstrated to improve the surgeon's understanding of intricate anatomical spatial-relationships (13), particularly following significant patho-anatomical deformation (14), and facilitate identification of "hidden" anatomical anomalies (12) not easily visible on conventional radiography. In such cases models were used preoperatively to determine operative feasibility and enable planning through selection or preparation of the most appropriate surgical technique for the individual presentation (approach, margins of resection, reconstruction options/strategies, necessary instrumentation).

Simulated surgery on the anticipated case anatomy represents a progression of biomodel applications in pre-surgical planning, whereby the haptic biomodel is used for practice and experimentation of procedural manoeuvres. Stereotaxy is a widely adopted technique used for intra-operative navigation (15). Biomodels have similarly been adopted for surgeon training and teaching purposes, whereby the design flexibility in terms of geometry and material properties (tissue density, hardness, flexibility) enables simulation of a range of clinical scenarios for surgical training (16,17) or anatomical learning (18) without the associated ethical and cost barriers, as well as anatomical variation, that can be present in cadaveric study.

Current 3DP technologies and biomodelling applications in spine

Biomodel design and manufacturing methods

Medical imaging to CAD

The workflow for creation of an anatomical biomodel involves, in general terms, initial acquisition of high-resolution patient imaging, computed tomography (CT) and/or magnetic resonance imaging (MRI), followed by segmentation, interpretation and 3D iso-surface reconstruction of the collated anatomical data to form a virtual model (19-26). Input into Computer-Aided design (CAD) software enables manual geometrical modifications and generation of the STereoLithography (.stl) file type suitable for 3DP. 3DP is used to manufacture the final physical construct through repetitive layer-by-layer deposition and fusion of raw printing materials derived from sequential CAD-model cross-sections and tool path generation (1,27).

3DP technologies

Three additive manufacturing processes are currently used to fabricate the majority of anatomical models:

Fused Deposition Modelling (FDM), Powder Bed Fusion (PBF) and Stereolithography Laser Curing (SLC). The fundamental differences in printing methods and compatible materials between these 3D printers causes inherent differences in the output properties and, therefore, functionality of the models produced. Biomodels made of nylon polymers are typically manufactured using PBF techniques, whereby the successive layers are formed by fusion of small substrate particles (powder beads) by high-powered laser. Although currently a comparatively expensive technique, the PBF method results in relatively high precision parts in materials such as nylon that are suitable for sterilisation, and therefore handling within the surgical sterile field. SLC is used to manufacture resin-based models and is dependent upon laser polymerisation of photo-initiated resins. SLC printed models are characteristically highly precise. FDM or Fused Filament Fabrication (FFF), which operates via melting and setting of extruded thermoplastics (such as acrylate) by the printer, is comparatively inexpensive, however produces the least precise models. Due to the lower cost barrier, FFF model production and testing has been wide spread with FFF models having well understood and useful mechanical properties for manipulations during surgical rehearsal (such as drilling and screw placement) (28).

Clinical benefits

Tack *et al.*'s (29) systematic review of surgical applications for 3DP found model use for preoperative planning and rehearsal in orthopaedic, maxillofacial and neurosurgery was associated with improvements in surgical workflows and postoperative patient outcomes. Reported reductions in operative time and duration of fluoroscopy potentially lower the risk of surgical site infection (30,31) and radiation exposure, while providing cost-offsets through improved operative-room ergonomics (27,32) and fewer post-surgical interventions (12).

Reduction of risk

Surgical intervention inherently poses a number of risks to a patient including risk of: infection, blood loss, excess tissue trauma due to imprecise surgical technique/approach, time spent under anaesthesia and exposure to ionising radiation. The risk of adverse events occurring during surgery is perhaps increased in spine surgery compared to general orthopaedic surgery due to the proximity of central nervous system neurological structures, which have very limited scope for repair (self or surgical), combined with the proximity of major arteries, including the aorta, iliac arteries (thoracic and lumbar spine), vertebral and carotid arteries (cervical). Biomodelling can aid the surgical team decision making and planning provided the biomodels used are accurate (precise, or reliable, and true, or valid) representations of the patient's anatomy (33). For example, decisions over the surgical approach can be made with better knowledge of the precise location of major vessels (see *Figures 1*,*2*). This is of particular use in the lumbar region, where the bifurcation of the aorta and trajectory of the vena cava varies from patient to patient (*Figure 2*). Additionally, tumours frequently alter and/or sequester blood vessels from nearby major vessels, meaning that there can be unusual/unexpected vessels that can cause bleeds if cut/torn during surgical resection of the tumour mass (*Figure 1*). High flow bleeds resulting from high pressure arteries can be problematic during surgery as not only do they increase the blood loss for the patient, and potentially complicate the anaesthesia, but they also add time and cost to the surgery as additional haemostatic agents may be required to stem the flow, before additional high speed, and thereby inherently risky, tissue resection is performed to find, isolate and repair the cut/torn vessel. Biomodels used in combination with virtual simulation of soft tissues can aid the neurosurgical, anaesthetic and, when working together, vascular team to avoid unexpected bleeds and/or prepare for the possibilities of them (*Figure 1*).

Biomodels have also demonstrated utility as an aid for preoperative patient education, improving patient understanding and their capacity to provide informed consent (34,35), thereby potentially reducing legal risks to surgeons in the case where adverse events occur to a patient following surgical intervention.

Effects of biomodel use in spine surgical workflow

In addition to pre-operative understanding of the pathology, combined with communication of the pathology and decision making by the surgical team (combined anaesthetic, neurosurgeon, vascular), the use of biomodels can aid the intra-operative workflow in a number of ways.

Reduced fluoroscopic events

Many reconstructive neurosurgical procedures involve the use of hardware/devices (7,19-22,36). Correct placement of devices is essential for the device to perform and

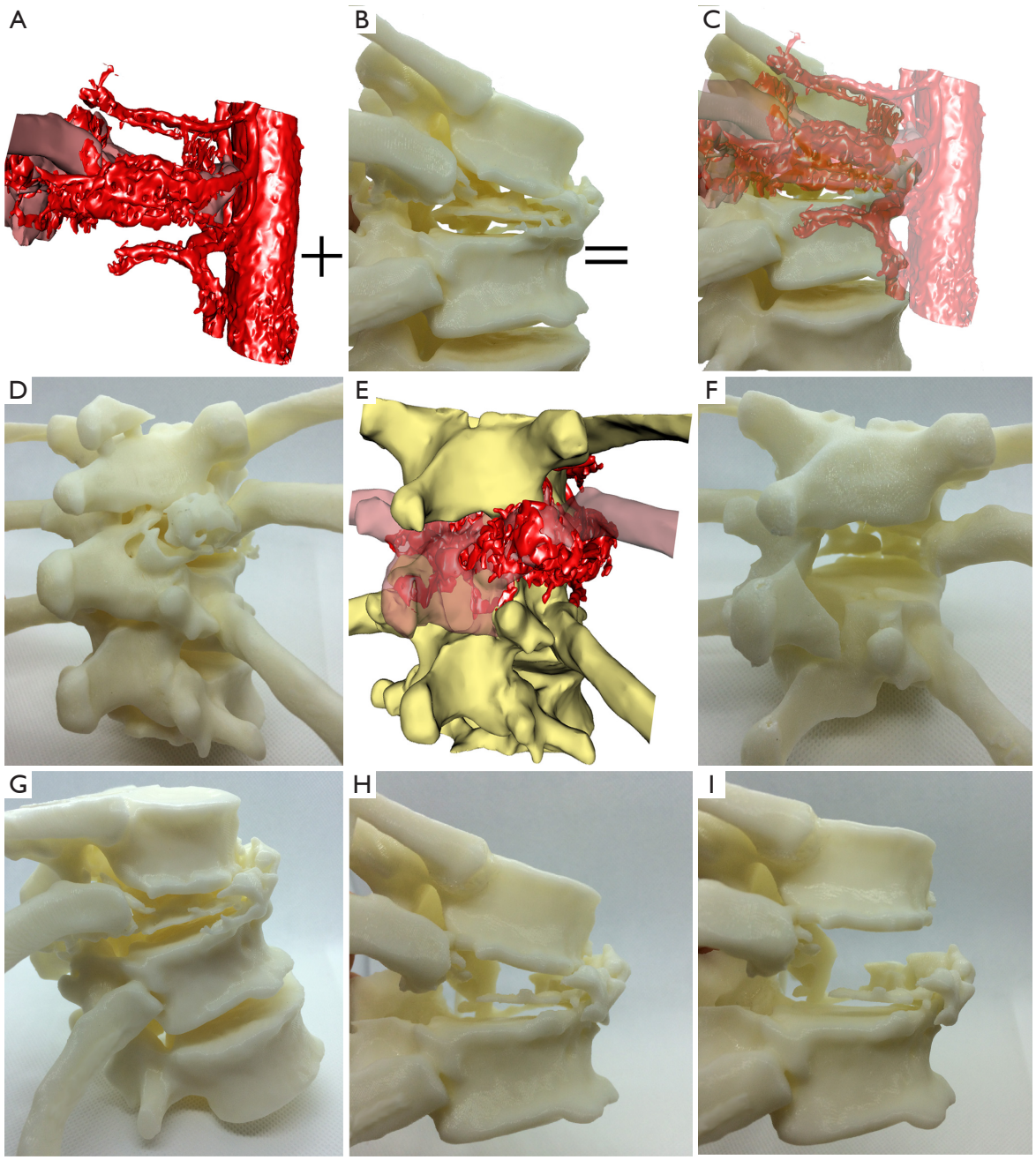

Figure 1 Virtual (in-silico) and physical (3DP) biomodels of a thoracic vertebral tumour. (A) Virtual modelling of the pathological bone (dull red) and surrounding vascular structures (bright, shiny red). The aorta runs vertically; (B) the 3DP model of the osteological anatomy showing the lytic effects of the tumour have caused kyphosis and compression; (C) virtual modelling of structures that may not be easy to print can add information and aid understanding in complex cases. In the case shown, the anterior osteology is fused and would need to be released in order to restore normal alignment to the spine. The addition of the vascularity makes it clear that the bone that would need cutting/nibbling is immediately adjacent to the aorta; (D) pre-operative state 3DP; (E) virtual model of the same as D with vascularity added. Understanding where the major vessels feeding the tumour mass can aid in planning the resection and understanding where and when bleeds may occur; (F) 3DP model of a possible resection using a posterior approach; (G) sagittal view of the pre-operative pathological state; (H) sagittal view of the result of the possible posterior resection plan; (I) a dynamic model allows for planning of reconstruction device height and size, as well as better planning of how the device can be inserted using the approach (see F).

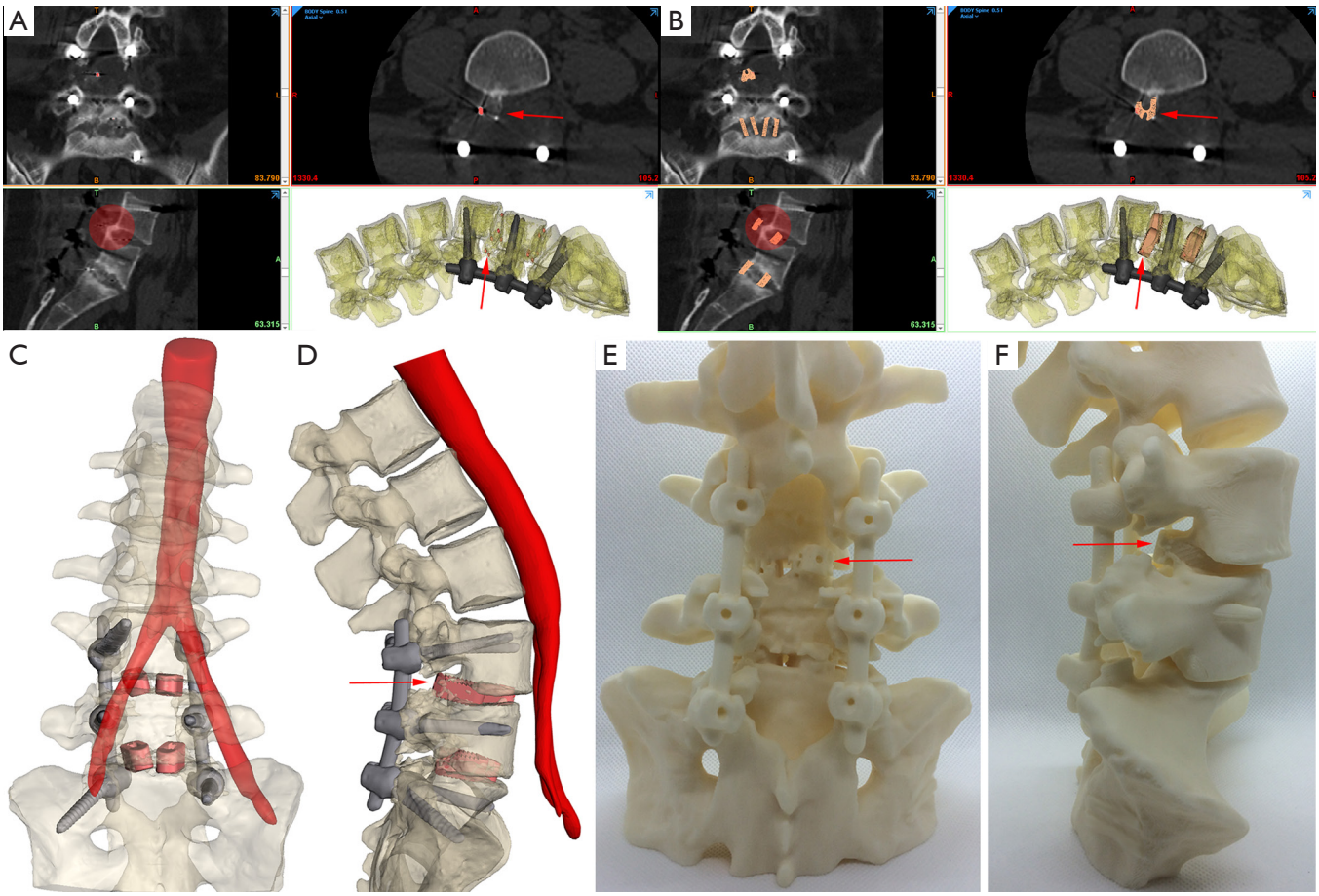

Figure 2 Complex revision surgery planning for lumbar spine L4–L5 and L5–S1 levels using virtual and 3DP biomodelling. The patient previously had procedures using posterior approaches with the aim of stabilising and fusing L4–S1. Laminectomies had been performed with posterior pedicle rods and screws placed L4–S1 (E). Two PEEK PLIFs were positioned in each of the L4–L5 and L5–S1 interbody spaces. Fusion had not occurred at either level with the graft windows of the PEEK devices largely devoid of bone and subsidence of the L5–S1 devices visible. Loosening of the pedicle screws had resulted in an L4–L5 spondylolisthesis. In addition, the right hand side L4–L5 PLIF device had backed out from the interbody space into the spinal canal. Arrows and translucent circles show the position of the backed out PLIF. (A) PEEK implants are invisible in the CT imaging and 3D reconstruction apart from embedded marker beads (shown in red), as indicated by the red arrows; (B) shows virtual PLIF cage placement in the CT. The red arrows indicate the same positions as in A but now with the virtual PLIF cage positioned in the CT and visible in the 3D reconstruction; (C) shows lumbar and sacral bone (translucent), aorta bifurcation to left and right iliac arteries, posterior rods and screws (black) virtual placement of PLIFs (light red) from an anterior viewpoint; (D) shows lateral viewpoint of the same as (C). The backed out right hand side L4–L5 PLIF indicated by the red arrow in D, E and F. The right hand L5 pedicle screw protrudes from the anterior surface of the L5 vertebral body (D and F) and has a trajectory coincident with the right iliac artery. Virtual reconstruction allows the distance between the L5 right hand screw tip and the iliac artery to be measured (12 mm). (E) Physical 3DP model included the reconstructed PLIF cages. The posterior viewpoint shows the result of the laminectomies as well as the right hand side L4–L5 PLIF backout. (F) 3DP model sagittal viewpoint in which the RHS backout PLIF is clearly visible, as is the protrusion of the RHS L5 pedicle screw. Revision surgery used an anterior approach to place ALIF devices. Biomodelling was used to aid with the surgical approach (vascular team) including iliac artery retractor placement with respect to the L5 screw protrusion as well as the removal of the PLIFs and insertion of the ALIF devices (neurosurgical team). The modelling showed that the spondylolisthesis at L4–L5 and large degree of lumbar lordosis kept the RHS iliac artery away from the L5 pedicle screw tip. PLIF, posterior lumbar interbody fusion; ALIF, anterior lumbar interbody fusion.

function as intended (20-22,37). Device placement is usually checked/confirmed by intra-operative fluoroscopy according to the surgical technique/instructions for use supplied with the device(s) (19-22). Pre-operative trial fitting of devices with biomodels can aid the surgical team identify haptic, for example the 'butting' of the device against a bony ridge, and/or anatomical or existing hardware landmarks or features that can aid in determining when the desired/planned position of the device has been achieved (*Figures 3*,*4*) (21,22). This can reduce the number of fluoroscopic imaging cycles required intra-operatively. An X-ray fluoroscopy cycle usually involves some or all of the following: the surgical team discontinuing surgical work; covering the incision(s) with sterilised drapes; a radiographer being called to the operating room; the radiographer positioning the X-ray device whilst the surgical team either huddle behind a radiation screen or exit the theatre; imaging, checking, re-alignment and re-imaging of the patient in one or more plane; moving the imaging equipment out of the sterile field; uncovering of the incision; re-commencement of surgery. Fluoroscopic events as described increase risk to the patient in a number of ways. As well as the direct risks associated with exposure to ionising radiation and prolonged anaesthesia, there are also risks associated for the surgical team exiting the sterile field and/or operating theatre (38). Operating theatres are typically under positive air pressure (39), with filtered clean air flowing down over the sterile field and out of the theatre through designed air-flow pathways (39). Pressure and flow of clean air are usually optimised for the sterile field (39), where the scrubbed in surgical team and theatre staff are, and optimal at the point where the patient will be positioned on the surgical table. Movement of the surgical team out of this area of the cleanest air introduces risks of airborne pathogens landing on a surgical team member's scrubbed region, and later being introduced to the patient's incision. Exiting the theatre altogether likely increases this risk further as well as introducing the risk of air borne pathogens being introduced into the theatre through opening of theatre doors (38-41). Therefore, minimisation of fluoroscopy cycles through identification of haptic cues and alignment of visual landmarks identified through preoperative use of biomodels can reduce these risks of infection, prolonged anaesthesia and ionising radiation to the patient.

Preoperative sizing of devices

In addition to correct placement of devices, selection of the correct size and angle of device to achieve the desired surgical reconstructive outcomes, such as decompression of neurology and restoration of sagittal balance, can be aided by the use of dynamic and/or pliable biomodels. Although virtual prediction of reconstruction can be performed, this process may be unfamiliar, and thereby less informative, to a surgical team (21). Instructions for use for many devices recommend insertion of trial, or sizer, devices before insertion of the final device. Due to the proximity of many devices to sensitive neurological structures (spinal cord, exiting nerve roots) the number of device insertion cycles, trial or final, should ideally be minimised as every insertion event carries some inherent risk. Anterior interbody fusion interventions are a relevant example of operating adjacent to sensitive structures (42). Hence, trialling of device dimensions on biomodels pre-operatively to reduce the number of device insertion cycles intra-operatively can reduce operating theatre time as well as reduce risk to the patient (*Figures 3*,*4*).

Dynamic biomodels can move either through replication of anatomical articulations or through material elastic/plastic deformation and can aid in assessment of the consequences of device insertion. For example, frequently the posterior elements such as the spinal processes, may be very close together and the introduction of an anterior interbody device with too much angulation may cause the spinal processes of adjacent levels to touch, which may cause posterior element pain for the patient post-operatively. This is particularly the case in degenerative patients, where osteophyte growth and reduction of inter-body height can decrease the distance between posterior elements of adjacent levels. In the case where a high/tall anterior device is used, the facets of the instrumented level may become overly distracted causing postoperative facetogenic pain (43). An oversized and/or point loaded implant also has an increased risk of subsidence (44,45). Identifying these factors intra-operatively is difficult and potentially time consuming as different trial devices are repeatedly inserted.

Use in combination with implants

Spinal device application is complicated by the numerous intervertebral articulations (anterior disc and posterior facets at each level) that may compound movements intra-operatively and thus reduce accuracy of the plan, a problem that can be reduced with the use of dynamic models (see below and *Figures 1*,*3*,*4*). Models enable trialling of spinal screw placement and identification of optimal screw trajectory, length and diameter prior to surgery, thus mitigating risks of iatrogenic neurovascular injury to the patient (*Figure 3*).

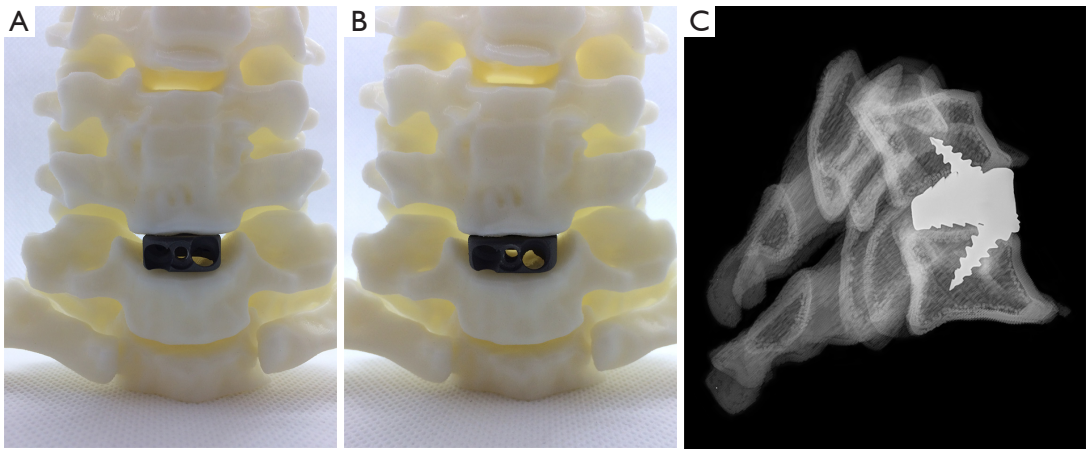

Figure 3 Pre-operative trialling of device sizes using a dynamic biomodel, shown in the C6–C7 interbody space (A and B). (A) 15 mm wide device, (B) 17 mm wide device; (C) sagittal plane X-ray of a physical 3DP biomodel (C5 and C6) used to test the fit of a cervical patient specific implant. X-ray allows screw trajectory and screw length to be assessed—in this case longer screws could safely be used.

Planning of placement and trajectory of tap holes for pedicle screws has benefitted from biomodelling (5,46). Biomodels combine naturally with 3DP drill jigs as a low cost barrier-to-entry alternative to robotic or image guided navigation (5). Biomodels can also be useful in decision making around anterior approach distraction (Caspar) pin placement and trajectory, particularly in revision and/or supplementary/secondary surgeries where existing hardware, such as an anterior plate, may prevent the usual pin placement and/or trajectory (*Figure 3*). Our team has found biomodelling useful in such instances as the model has allowed not only the placement and trajectory of the distraction pins to be planned, which has influenced the surgical approach (placement and extents of the soft tissue incision), but also the planning of how the distraction pins may interact with other instrumentation during different stages of the procedure, thereby allowing better planning of the surgical workflow including locating and preparing the instrumentation necessary for an anterior plate removal. In particular, biomodels have benefitted cases where previous instrumentation, such as cervical anterior plate and screws, have been removed whilst an adjacent level has undergone ACDF (*Figure 4*). The combination of preparing all of the necessary instrumentation and determination of the optimal surgical workflow prior to the procedure is estimated to save 30–45 minutes in the operating theatre depending on anatomical and case complexity.

Complex pathology/trauma/tumour resection

Visualisation and haptic manipulation of a patient-specific biomodel in a 1:1 scale to the structures it is designed to replicate provides more intuitive appreciation of regional anatomy and enhances opportunity for interpretation of associated pathologies than planar radiographic imagery or two-dimensional representations of digital renders. This is particularly useful for cases of significant surgical complexity, such as where anatomical deformation due to neoplasia, traumatic injury or congenital anomaly mandate extensive preoperative consideration to identify the appropriate approach or patient positioning, surgical techniques, margins and extent of resection necessary and reconstructive strategies. In such cases biomodels can be made in which the pathological portion of anatomy for surgical resection can be fabricated as a separate entity, which can be assembled and disassembled with the non-pathological anatomy (22).

Other biomodel properties

Colour

The use of colour in biomodels can aid communication of pathology or structures (anatomical or otherwise) of importance to the case. For example, the pathological portion of a model assembly can be a different colour to the normal portion of the model (22). Colour can also be used to highlight regions/structures of interest, such as blood vessels or the 3D extents of a tumour (*Figure 1*). Where the tumour is encapsulated within the bone margins, a clear model with a coloured tumour region can be particularly effective/useful (*Figure 5*). The colouring of the tumour

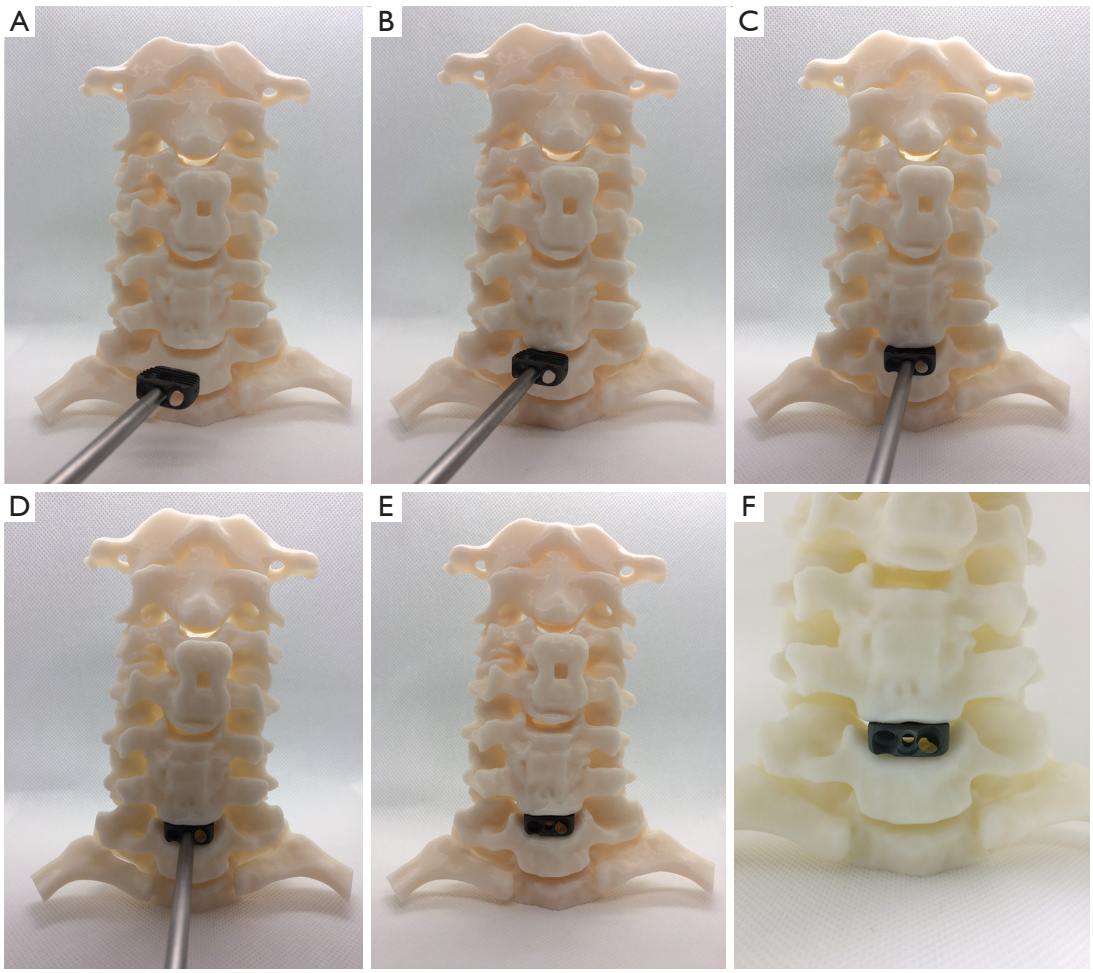

Figure 4 Process of device trialling using a dynamic biomodel (A,B,C,D,E) and the resulting fit of the device in the C6–C7 interbody space (F). The device inserter can be used (as shown in A,B,C,D,E) to aid in the trialling/planning process. Note that the model shows two previous fusions at C3–4 (with anterior plate) and C5–6. This biomodel was used to plan the removal of the anterior plate as well as an additional fusion and disc replacement. The model aided the surgical team in preparing the revision instrumentation for the plate removal, where the Caspar pins for the C2–C3 level distraction would insert once the C3–4 plate was removed, plan the trajectory to accommodate these steps, as well as plan the order of the procedure (surgical workflow planning). The surgical workflow planning along with the device trialling was estimated to have saved 30–45 min of time in the operating room.

regions can be representative of the MRI signal intensity. Differential colouring representative of MRI or other scan signals can aid in planning biopsy approach and/or regions/limits of surgical incisions as hotter colours of strongest MRI signals can indicate to a surgeon where the tumour is most active, which may be the tumour region from which biopsy/pathology results will be most informative (*Figure 5*).

Accuracy

In our view, it is essential that patient specific biomodels provided to health care practitioners are accurate to the anatomy. Accuracy is defined as a combination of trueness (or validity) and precision (or reliability) (33). Precision is limited by CT scan 'resolution', where resolution is a combination of pixel size and slice thickness. A high resolution medical CT scan usually has a pixel size between 0.2–0.4 mm and slice thickness of between 0.2–3.0 mm. For scans with higher slice thicknesses of 1.0–3.0 mm or more (for both MR and CT), the CAD thresholding, segmentation and interpretation stages of the biomodelling process may take longer and need more skill and anatomical familiarity. A single threshold value applied to a CT will likely not

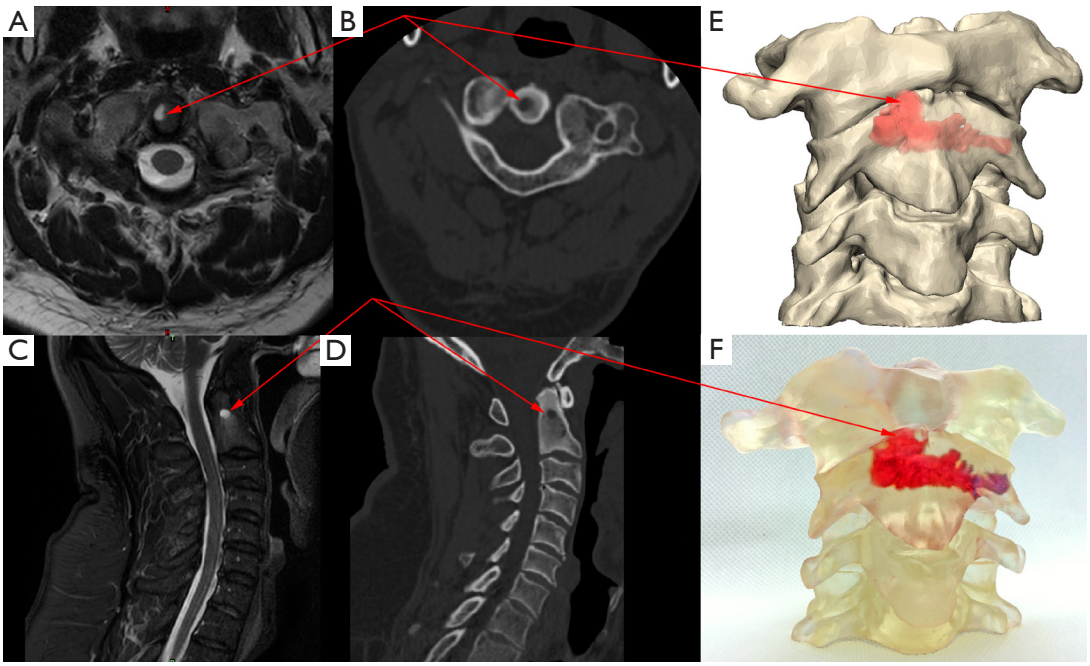

Figure 5 Medical imaging, virtual reconstruction and physical manifestation of C2 vertebral body tumour. (A) and (C) are axial and sagittal (respectively) T2 weighted MRI slices showing the 'hot spot' of tumour activity; (B) and (D) show axial and sagittal (respectively) CT slices in the same positions as (A) and (C) showing the lesion; (E) virtual reconstruction of cervical osteology (C1-midway C4) anatomy showing internal lesion (red); (F) 3DP clear model of E with the lesion coloured according to MRI signal—brighter red associated with high intensity of MRI signal, blue/purple associated with lower intensity MRI signal.

result in a true representation of the anatomy, particularly where pathology or instrumentation from previous surgical intervention is present, or where the bone mineral density is low. In such cases a single threshold value applied to a CT will usually lead to a 3D model in which there are holes in the vertebral bodies, transverse processes and spinal processes. These holes are areas of low mineralisation in the bone or where there is a very thin cortical layer, perhaps well below the pixel size, but are not likely actual holes in the bones. Converting a single threshold value segmentation to a 3D model and printing this will give an untrue, and therefore inaccurate, representation of the anatomy. Training, skill and care are needed to interpret what the scan data truly represents in terms of patient anatomy. An inaccurate biomodel may be, at best, less useful for the health care professional and at worst, misleading, which could lead to misinterpretation of the patient's anatomy and a sub-optimal surgical plan.

Sterility

If a biomodel is required to enter the sterile field, then the biomodel needs to be validated for cleaning and sterilisation and potentially manufactured from a material that is biocompatible (47). Difficulties in validating suitability for sterilisation exist for more geometrically complex models, for example where an internal lattice structure is used to reduce material use in the model, as is typical for FDM/FFF models, or where lytic tumours have created complex internal cavities within the bone. Geometrical complexity makes cleaning and sterilisation validation more difficult as it is difficult to define the boundaries/limits of geometric complexity for such models in order to define worse case scenarios for cleaning and sterilisation validation testing.

Value

Reductions in surgery times provide value to health care providers (hospitals) as operating theatres are expensive to run. Reductions in procedure time can result in realisation of added value to health care providers. However, it is difficult to obtain precise costs of running an operating theatre per hour/minute either for United States of America

(US) or Australian (AUS) hospitals (48-50). Shippert [2005] analysed US hospital and anaesthetic groups and found a range of US$21.80 to US$131.12 per minute operating room fees, with an additional US$2.20–US$6.10 per minute anaesthetist fees (50). Macario [2010] identified the difference between cost (what it actually costs the hospital to run the operating theatre) and charge (what the hospital charged payers—patients or health funds based on list [Prosthesis list in Australia] prices) (48). Macario also found that there are no published definitive figures for operating room costs, but that these could likely be estimated at US$15–$20 per minute (in 2010) (48). Charges were reported to vary depending on case complexity (US $29 per minute to $80 per minute excluding anaesthetic charges), which likely relates to underlying cost differences. Shippert found that time-cost efficiency was seen in disposable rather than reusable devices and with products that required fewer steps for their use/application. Shippert stated and that to save over US$100,000 each surgeon needed to save ~7 minutes per procedure on 250 cases (50). For major surgeries such as the spinal procedures discussed herein, 250 device implantation procedures would represent a relatively high volume of cases to be performed within a year. Shippert's figures equate to ~21 minutes per procedure for 68 cases, or slightly over 1 complex case per week.

The Australian health system is state based. The cost of running operating theatres in the state of NSW, as of 2014, has not been accurately defined (49). The Queensland Audit Office [2016] provides figures that equate to AUD$8,525.17 per hour, or AUD$142.09 per minute for operating theatre running costs for the year 2014–2015 (51), which is within Shippert's findings adjusted to current currency values US$28.66–US$172.38 being equivalent to AUD$34.61–AUD$208.19 (assuming no change in the underlying costs and using an average (year end since 2005) currency rate of AUD $1.21 : US$1 with an overall inflation rate of 1.3147 since 2005). Shippert [2005] simply concluded that saving operating time saved money as well as reducing risk to the patient (50). To recoup the UAD$1,950 Australian prosthesis list cost for a biomodel (52), the hospital would need to save 13.72 minutes of operating room time.

Conclusions

The current review supports biomodelling to assist the surgeon and surgical team, to understand better and deal with complex anatomy and pathologies encountered during surgical practice, and as a useful and at times essential tool in the armamentarium of imaging techniques used for complex spinal surgery.

Acknowledgments

None.

Footnote

Conflicts of Interest: WCH Parr and RJ Mobbs declare share holdings in 3DMorphic. The other authors have no conflicts of interest to declare.

Ethical Statement: The authors are accountable for all aspects of the work in ensuring that questions related to the accuracy or integrity of any part of the work are appropriately investigated and resolved.

References

1. Rengier F, Mehndiratta A, Von Tengg-Kobligk H, et al. 3D printing based on imaging data: review of medical applications. Int J Comput Assist Radiol Surg 2010;5:335-41.
2. Wilcox B, Mobbs RJ, Wu AM, et al. Systematic review of 3D printing in spinal surgery: the current state of play. J Spine Surg 2017;3:433-43.
3. Lu S, Xu YQ, Lu WW, et al. A novel patient-specific navigational template for cervical pedicle screw placement. Spine 2009;34:E959-E966.
4. D'Urso PS, Williamson OD, Thompson RG. Biomodeling as an Aid to Spinal Instrumentation. Spine 2005;30:2841-5.
5. Kim J, Rajadurai J, Choy WJ, et al. Three-Dimensional Patient-Specific Guides for Intraoperative Navigation for Cortical Screw Trajectory Pedicle Fixation. World Neurosurg 2019;122:674-9.
6. Phan K, Sgro A, Maharaj MM, et al. Application of a 3D custom printed patient specific spinal implant for C1/2 arthrodesis. J Spine Surg 2016;2:314-8.
7. Burnard JL, Parr WCH, Choy WJ, et al. 3D-printed spine surgery implants: a systematic review of the efficacy and clinical safety profile of patient-specific and off-the-shelf devices. Eur Spine J 2019. [Epub ahead of print].
8. Choy WJ, Mobbs RJ, Wilcox B, et al. Reconstruction of Thoracic Spine Using a Personalized 3D-Printed Vertebral Body in Adolescent with T9 Primary Bone Tumor. World Neurosurg 2017;105:1032.e13-1032.e17.
9. Choy WJ, Parr WCH, Phan K, et al. 3-dimensional

printing for anterior cervical surgery: a review. J Spine Surg 2018;4:757-69.
10. D'Urso PS, Askin G, Earwaker JS, et al. Spinal Biomodeling. Spine 1999;24:1247-51.
11. Yap YL. 3D printed bio-models for medical applications. Rapid Prototyping Journal 2017;23:227-35.
12. Izatt MT, Thorpe PLPJ, Thompson RG, et al. The use of physical biomodelling in complex spinal surgery. Eur Spine J 2007;16:1507-18.
13. Wurm G, Tomancok B, Pogady P, et al. Cerebrovascular stereolithographic biomodeling for aneurysm surgery. J Neurosurg 2004;100:139-45.
14. The utility of 3D printing for surgical planning and patient-specific implant design for complex spinal pathologies: Case report. J Neurosurg Spine 2017;26:513-8.
15. Kalfas IH, Kormos DW, Murphy MA, et al. Application of frameless stereotaxy to pedicle screw fixation of the spine. J Neurosurg 1995;83:641-7.
16. Waran V, Narayanan V, Karuppiah R, et al. Utility of multimaterial 3D printers in creating models with pathological entities to enhance the training experience of neurosurgeons. J Neurosurg 2014;120:489-92.
17. Shiraishi I, Yamagishi M, Hamaoka K, et al. Simulative operation on congenital heart disease using rubber-like urethane stereolithographic biomodels based on 3D datasets of multislice computed tomography. Eur J Cardiothorac Surg 2010;37:302-6.
18. McMenamin PG, Quayle MR, McHenry CR, et al. The Production of Anatomical Teaching Resources Using Three-Dimensional (3D) Printing Technology. Anat Sci Educ 2014;7:479-86.
19. Joffe MR, Parr WCH, Tan C, et al. Development of a Customized Interbody Fusion Device for Treatment of Canine Disc-Associated Cervical Spondylomyelopathy. Vet Comp Orthop Traumatol 2019;32:79-86.
20. Mobbs RJ, Choy WJ, Wilson P, et al. L5 En-Bloc Vertebrectomy with Customized Reconstructive Implant: Comparison of Patient-Specific Versus Off-the-Shelf Implant. World Neurosurg 2018;112:94-100.
21. Mobbs RJ, Parr WCH, Choy WJ, et al. Anterior Lumbar Interbody Fusion (ALIF) using a personalised approach: Is custom the future of implants for ALIF surgery? World Neurosurg 2019. [Epub ahead of print].
22. Parr WCH, Burnard JL, Singh T, et al. Cervical 3-5 Chordoma resection and reconstruction with a 3D printed Titanium Patient Specific Implant: a case report. World Neurosurg 2019. [Epub ahead of print].
23. Parr WCH, Wroe S, Chamoli U, et al. Toward integration of geometric morphometrics and computational biomechanics: New methods for 3D virtual reconstruction and quantitative analysis of Finite Element Models. J Theor Biol 2012;301:1-14.
24. Singh T, Parr W, Choy WJ, et al. Three-Dimensional Morphometric Analysis of Lumbar Vertebral Endplate Anatomy. World Neurosurg 2019. [Epub ahead of print].
25. Tan CJ, Parr WCH, Walsh WR, et al. Influence of Scan Resolution, Thresholding, and Reconstruction Algorithm on Computed Tomography-Based Kinematic Measurements. J Biomech Eng 2017. doi: 10.1115/1.4037558.
26. Wroe S, Parr WCH, Ledogar JA, et al. Computer simulations show that Neanderthal facial morphology represents adaptation to cold and high energy demands, but not heavy biting. Proc Biol Sci 2018. doi: 10.1098/rspb.2018.0085.
27. Ventola CL. Medical applications for 3D printing: current and projected uses. P T 2014;39:704-11.
28. Jap NSF, Pearce GM, Hellier AK, et al. The effect of raster orientation on the static and fatigue properties of filament deposited ABS polymer. Int J Fatigue 2019;124:328-37.
29. Tack P, Victor J, Gemmel P, et al. 3D-printing techniques in a medical setting: a systematic literature review. Biomed Eng Online 2016;15:115.
30. Pull ter Gunne AF, Cohen DB. Incidence, prevalence, and analysis of risk factors for surgical site infection following adult spinal surgery. Spine 2009;34:1422-8.
31. Arts MP, Peul WC. Vertebral Body Replacement Systems with Expandable Cages in the Treatment of Various Spinal Pathologies: A Prospectively Followed Case Series of 60 Patients. Neurosurgery 2008;63:537-44; discussion 544-5.
32. Thayaparan GK, Owbridge MG, Thompson RG, et al. Designing patient-specific 3D printed devices for posterior atlantoaxial transarticular fixation surgery. J Clin Neurosci 2018;56:192-8.
33. Streiner DL, Norman GR. "Precision" and "Accuracy": Two Terms That Are Neither. J Clin Epidemiol 2006;59:327-30.
34. Liew Y, Beveridge E, Demetriades AK, et al. 3D printing of patient-specific anatomy: a tool to improve patient consent and enhance imaging interpretation by trainees. Br J Neurosurg 2015;29:712-4.
35. Bernhard JC, Isotani S, Matsugasumi T, et al. Personalized 3D printed model of kidney and tumor anatomy: a useful tool for patient education. World J Urol 2016;34:337-45.
36. Choy WJ, Parr WCH, Phan K, et al. 3-dimensional

printing for anterior cervical surgery: a review. J Spine Surg 2018;4:757-69.
37. Spetzger U, Frasca M, König S. Surgical planning, manufacturing and implantation of an individualized cervical fusion titanium cage using patient-specific data. Eur Spine J 2016;25:2239-46.
38. Perez P, Holloway J, Ehrenfeld L, et al. Door openings in the operating room are associated with increased environmental contamination. Am J Infect Control 2018;46:954-6.
39. Wang C, Holmberg S, Sadrizadeh S. Impact of door opening on the risk of surgical site infections in an operating room with mixing ventilation. Indoor and Built Environment 2019. DOI: 10.1177/1420326X19888276.
40. Andersson AE, Bergh I, Karlsson J, et al. Traffic flow in the operating room: An explorative and descriptive study on air quality during orthopedic trauma implant surgery. Am J Infect Control 2012;40:750-5.
41. Mathijssen NMC, Hannicnk G, Sturm PDJ, et al. The Effect of Door Openings on Numbers of Colony Forming Units in the Operating Room during Hip Revision Surgery. Surg Infect (Larchmt) 2016;17:535-40.
42. Mobbs RJ, Phan K, Malham G, et al. Lumbar interbody fusion: techniques, indications and comparison of interbody fusion options including PLIF, TLIF, MI-TLIF, OLIF/ATP, LLIF and ALIF. J Spine Surg 2015;1:2-18.
43. Kirzner N, Etherington G, Ton L, et al. Relationship between facet joint distraction during anterior cervical discectomy and fusion for trauma and functional outcome. Bone Joint J 2018;100-B:1201-7.
44. Kao TH, Wu CH, Chou YC, et al. Risk factors for subsidence in anterior cervical fusion with stand-alone polyetheretherketone (PEEK) cages: a review of 82 cases and 182 levels. Arch Orthop Trauma Surg 2014;134:1343-51.
45. Suh PB, Puttlitz C, Lewis C, et al. The Effect of Cervical Interbody Cage Morphology, Material Composition, and Substrate Density on Cage Subsidence. J Am Acad Orthop Surg 2017;25:160-8.
46. Mobbs RJ, Choy WJ, Singh T, et al. Three-Dimensional Planning and Patient-Specific Drill Guides for Repair of Spondylolysis/L5 Pars Defect. World Neurosurg 2019;132:75-80.
47. IMDRF. Essential Principles of Safety and Performance of Medical Devices and IVD Medical Devices. International Medical Device Regulators Forum; 2018.
48. Macario A. What does one minute of operating room time cost? J Clin Anesth 2010;22:233-6.
49. NSWGovernment. Operating Theatre Efficiency 2014. Available online: https://www.aci.health.nsw.gov.au/resources/surgical-services/efficiency/theatre-efficiency
50. Shippert RD. A Study of Time-Dependent Operating Room Fees and How to save $100 000 by Using Time-Saving Products. The American Journal of Cosmetic Surgery 2005;22:25-34.
51. QAO. Queensland public hospital operating theatre efficiency. In: Office QA. editor. 2015.
52. Australian Government. The Prostheses List. In: Health DO. editor. 2019.

Cite this article as: Parr WCH, Burnard JL, Wilson PJ, Mobbs RJ. 3D printed anatomical (bio)models in spine surgery: clinical benefits and value to health care providers. J Spine Surg 2019;5(4):549-560. doi: 10.21037/jss.2019.12.07